

Global Expression of Molecular Transporters in the Human Vaginal Tract: Implications for HIV Chemoprophylaxis

Manjula Gunawardana¹, Madeline Mullen¹, John A. Moss¹, Richard B. Pyles², Rebecca J. Nusbaum³, Jignesh Patel², Kathleen L. Vincent⁴, Charles Wang⁵, Chao Guo⁵, Yate-Ching Yuan⁶, Charles D. Warden⁶, Marc M. Baum^{1*}

¹Department of Chemistry, Oak Crest Institute of Science, 2275 E. Foothill Blvd., Pasadena, CA 91107, USA, ²Departments of Pediatrics and Microbiology and Immunology, UTMB. 301 University Blvd, Galveston, TX 77555, USA, ³Human Pathophysiology and Translational Medicine Graduate Program, UTMB. 301 University Blvd, Galveston, TX 77555, USA, ⁴Center for Biomedical Engineering, 301 University Boulevard, University of Texas Medical Branch at Galveston, TX 77555, USA, ⁵Functional Genomics Core, Beckman Research Institute, City of Hope Comprehensive Cancer Center, 1710 Flower Ave., Duarte, CA 91010, USA, ⁶Bioinformatics Core, Department of Molecular Medicine, City of Hope National Medical Center, 1500 East Duarte Rd., Duarte, CA 91010, USA.

Supplementary Materials

Fig. S1. Clustering of samples analyzed by Principal Component Analysis (PCA). Samples cluster primarily by subject, and no strong outliers are apparent. Subject ID: 1, red; 2, dark blue; 3, green; 4, purple; 5, orange; and 6, cyan.

Fig. S2. Dendrogram showing hierarchical clustering of vaginal samples. (A) Color bar indicates strong clustering among samples from the same subject, for subjects 1-6. Color bars defining clustering along the following axes in the vaginal tract (Fig. 1) show no discernible pattern: (B) anterior-posterior, (C) distal-proximal, and (D) left-right.

Fig. S3. Distribution of averaged expression patterns for membrane transporters. Average expression values per probe across samples ($N = 44$), sorted in descending order.

Fig. S4. Example of a transporter gene *SLC44A1* with universally high expression patterns in the TiGER database. Notice practically all of these tissues show some level of enrichment and there are no tissue-specific signatures (with enrichment score stronger than 5 for a particular tissue).

Fig. S5. Hierarchical clustering of membrane transporter expression across the anterior-posterior axis of the vaginal tract. (A) Color bars show increased clustering pattern along the anterior-posterior axis in the vaginal tract (Fig. 1), when compared to the clustering observed for all membrane transporters (Fig. 3 and Fig. S2). The heatmap shows clustering of the standardized expression values, where probes with high expression are shown in red and probes with low expression are shown in blue (see color key below the heatmap). *SLC46A1* and *SLC45A3* appear in a cluster that is up-regulated in anterior samples, while *SLC35F2*, *SLC9A1*, *SLC6A9*, and *SLC10A6* appear in a cluster that is up-regulated in posterior samples.

Fig. S6. Sources of variation in global gene expression. A-P, anterior-posterior axis; P-D, proximal-distal axis; and L-R, left-right. ANOVA was used to compare the above factors and F-statistics were calculated and averaged across all genes on the microarray. Average F-statistics for each variable were divided by the average F-statistic for unexplained variability (Error), and these ratios are shown in the figure. For example, the ratio for L-R is 1.18, meaning that this variable explained 18% more variation than would be explained by a 5th variable associated with

random noise. Likewise, the subject ID can explain approximately twice the variation observed for A-P.

Fig. S7. Sample histogram. An over-expression threshold of 3.5 was determined from this plot.

Table S1. Summary of 41 vaginal tissue sample number per location for each subject used in the differential gene expression analyses. The sample location in the vaginal tract is shown schematically in Fig. 1.

Table S2. Tissue-specific scores for highly expressed membrane transporters. Tissue-specific expression requires a score > 5 and P -value $< 10^{-3.5}$. N/A, gene not present in database.

Dataset S1. Over-expression and averaged expression data in tabular form for all molecular transporters.

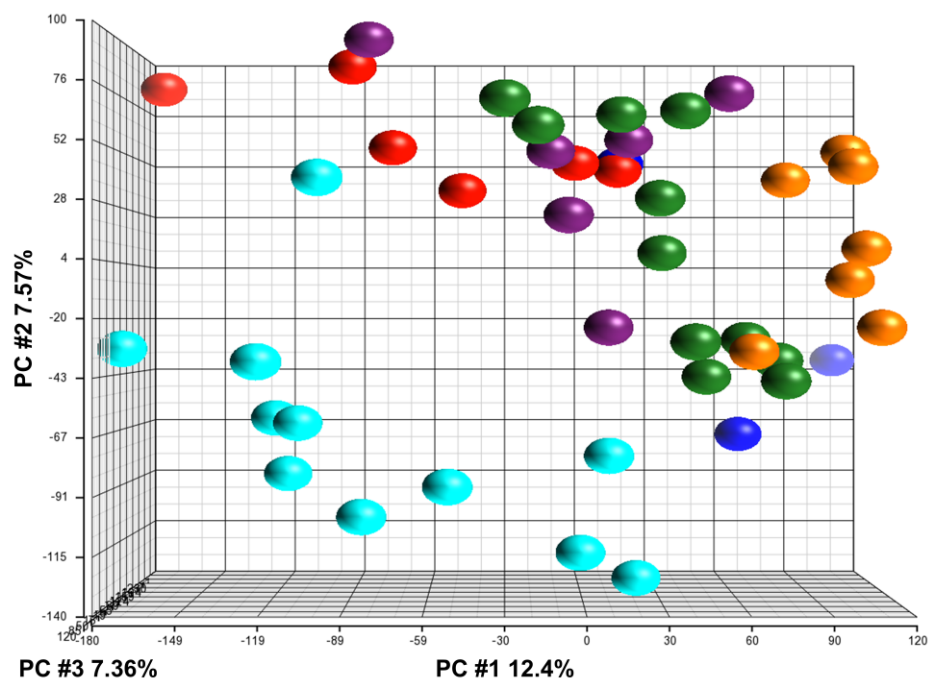


Fig. S1. Clustering of samples analyzed by Principal Component Analysis (PCA). Samples cluster primarily by subject, and no strong outliers are apparent. Subject ID: 1, red; 2, dark blue; 3, green; 4, purple; 5, orange; and 6, cyan.

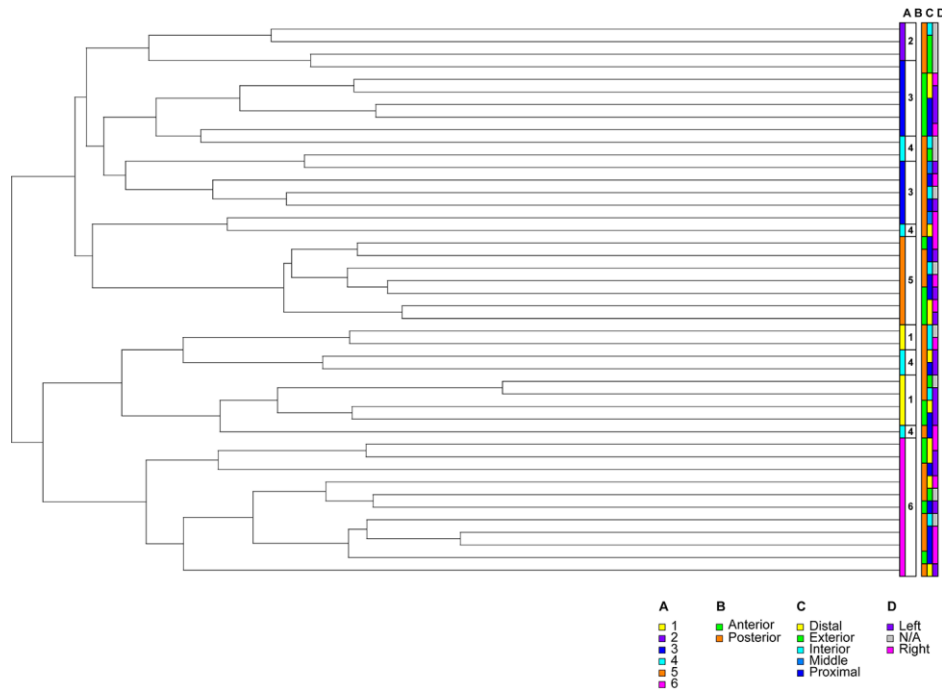


Fig. S2. Dendrogram showing hierarchical clustering of vaginal samples. (A) Color bar indicates strong clustering among samples from the same subject, for subjects 1-6. Color bars defining clustering along the following axes in the vaginal tract (Fig. 1) show no discernible pattern: (B) anterior-posterior, (C) distal-proximal, and (D) left-right.



Fig. S3. Distribution of averaged expression patterns for membrane transporters. Average expression values per probe across samples ($N = 44$), sorted in descending order.

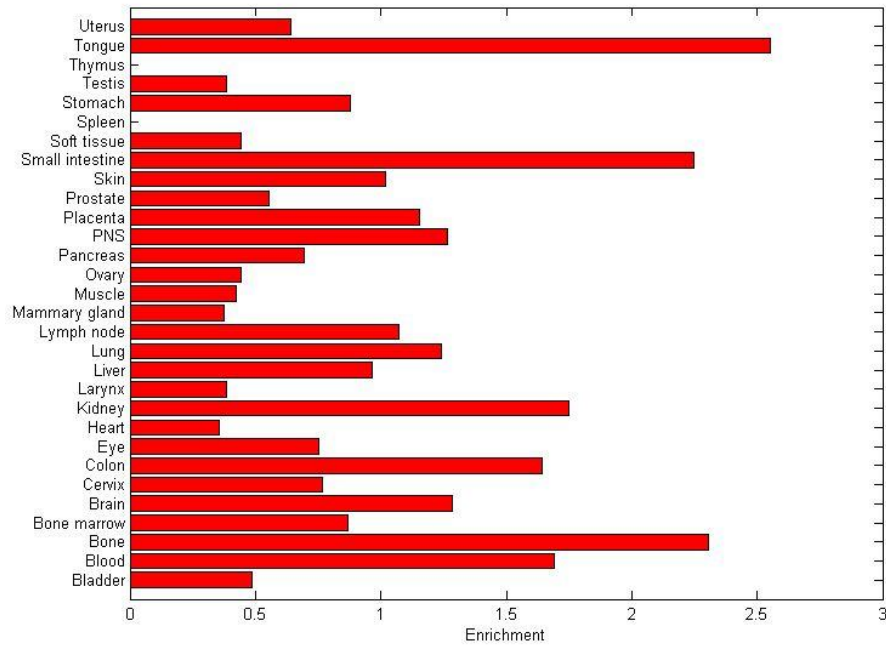


Fig. S4. Example of a transporter gene *SLC44A1* with universally high expression patterns in the TiGER database. Notice practically all of this tissues show some level of enrichment and there are no tissue-specific signatures (with enrichment score stronger than 5 for a particular tissue).

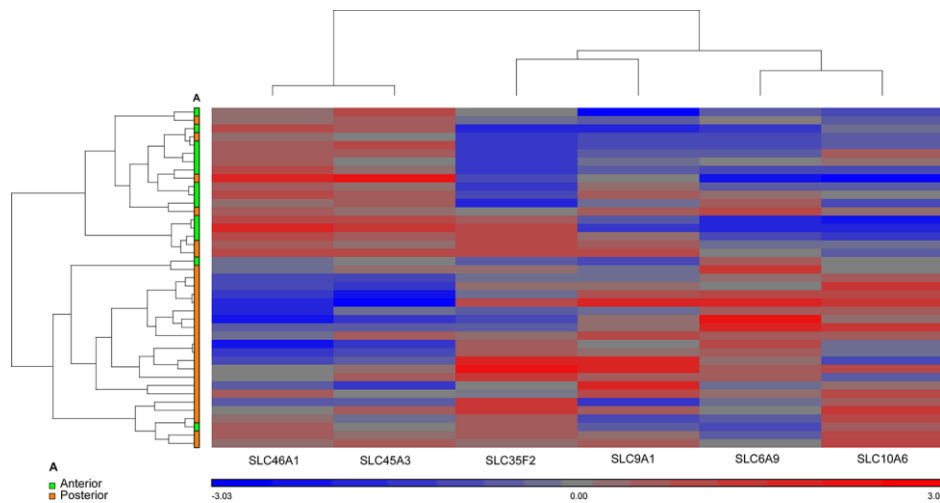


Fig. S5. Hierarchical clustering of membrane transporter expression across the anterior-posterior axis of the vaginal tract. (A) Color bars show increased clustering pattern along the anterior-posterior axis in the vaginal tract (Fig. 1), when compared to the clustering observed for all membrane transporters (Fig. 3 and Fig. S2). The heatmap shows clustering of the standardized expression values, where probes with high expression are shown in red and probes with low expression are shown in blue (see color key below the heatmap). *SLC46A1* and *SLC45A3* appear in a cluster that is up-regulated in anterior samples, while *SLC35F2*, *SLC9A1*, *SLC6A9*, and *SLC10A6* appear in a cluster that is up-regulated in posterior samples.

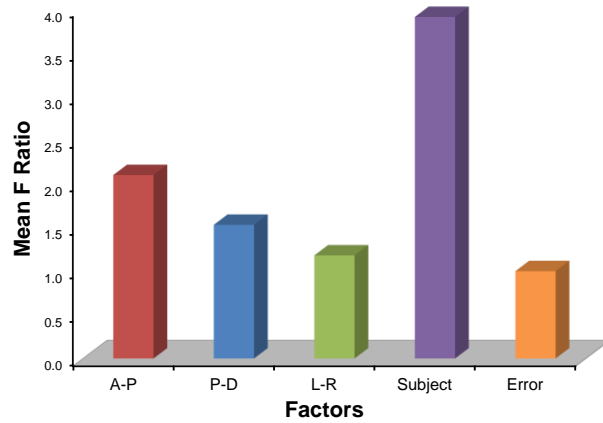


Fig. S6. Sources of variation in global gene expression. A-P, anterior-posterior axis; P-D, proximal-distal axis; and L-R, left-right. ANOVA was used to compare the above factors and F-statistics were calculated and averaged across all genes on the microarray. Average F-statistics for each variable were divided by the average F-statistic for unexplained variability (Error), and these ratios are shown in the figure. For example, the ratio for L-R is 1.18, meaning that this variable explained 18% more variation than would be explained by a 5th variable associated with random noise. Likewise, the subject ID can explain approximately twice the variation observed for A-P.

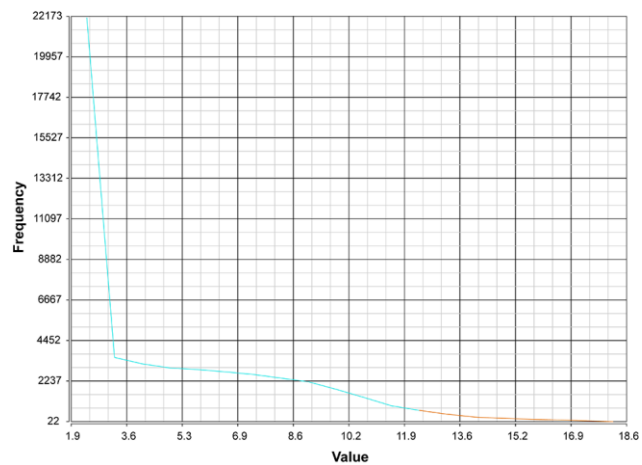


Fig. S7. Sample histogram. An over-expression threshold of 3.5 was determined from this plot.

Table S1. Summary of 41 vaginal tissue sample number per location for each subject used in the differential gene expression analyses. The sample location in the vaginal tract is shown schematically in Fig. 1.

Sample Location *	Subject ID					
	1	2	3	4	5	6
Anterior, proximal			2		2	2
Anterior, distal	2		2		2	2
Posterior, proximal			2	2	2	2
Posterior, distal			2 [†]	2		2
Posterior, interior	3	1	1	1	1	1
Posterior, exterior	1	1	1	1		1

*Usually collected from right and left side of vaginal wall.

[†]Identified as “posterior middle”.

Table S2. Tissue-specific scores for highly expressed membrane transporters. Tissue-specific expression requires a score > 5 and *P*-value < 10^{-3.5}. N/A, gene not present in database.

Gene Symbol	Tissue-specific Enrichment	Uterus Score	Ovary Score	Cervix Score
<i>RHCG</i>	larynx, tongue	0.24	0	1.0
<i>TAP1</i>	none	3.0	0.77	3.1
<i>SLC2A1</i>	none	0.46	1.7	0.58
<i>SLC6A9</i>	none	0	0	4.1
<i>SLC16A3</i>	none	0.48	2.3	2.3
<i>SLC16A12</i>	kidney, pancreas	0.94	0	0
<i>SLC22A18</i>	colon	0	0.42	0.98
<i>SLC24A3</i>	none	1.8	0	0
<i>SLC35E1</i>	none	1.4	1.3	0.84
<i>SLC35E4</i>	kidney, pancreas	0.94	0	0
<i>SLC44A1</i>	none	0.64	0.44	0.77
<i>SLC38A10</i>	N/A	N/A	N/A	N/A